Boundary-Layer Behavior on Continuous Solid Surfaces: III. The Boundary Layer on a Continuous Cylindrical Surface

B. C. SAKIADIS

E. I. du Pont de Nemours and Company, Incorporated, Wilmington, Delaware

The behavior of laminar and turbulent boundary layers on a moving continuous cylindrical surface is investigated by the integral method, based on assumed velocity profiles that satisfy the appropriate boundary conditions. Equations for the characteristic boundary-layer parameters are presented for both the laminar and turbulent boundary layers, and comparison is made with the boundary-layer behavior over a cylindrical surface of finite length. The analysis for the laminar boundary layer with a logarithmic velocity profile leads to satisfactory results. The turbulent boundary-layer behavior on continuous cylindrical surfaces, and cylindrical surfaces of finite length, can best be investigated experimentally.

In a previous paper (*19*) the boundary-layer behavior on continuous surfaces was examined and compared with the boundary-layer behavior on surfaces of finite length. In the same paper the differential equations of motion and boundary conditions that determine the fluid behavior were examined, and the integral momentum equations applicable to continuous surfaces were derived. The results of that study indicate that the known solutions for the boundary layer on surfaces of finite length are not applicable to the boundary layer on continuous surfaces.

In a subsequent paper (*20*) the boundary-layer equations were solved to determine the characteristics of the laminar and turbulent boundary layers on a continuous flat surface. The laminar boundary layer was investigated by two methods. One method involves the numerical solution, with appropriate boundary conditions, of the differential boundary-layer equations; the other involves the integral momentum equation of boundary-layer theory, based on an assumed velocity profile. The turbulent boundary layer was investigated by the integral momentum method only.

In this paper the boundary-layer equations will be solved to determine the behavior of laminar and turbulent boundary layers on a continuous cylindrical surface. Both the laminar and turbulent boundary layers will be investigated by use of the previously derived (*19*) integral momentum equation of boundary-layer theory. The characteristic boundary-layer parameters will be derived and compared with the corresponding parameters for a cylindrical surface of finite length. The present state of theoretical and experimental knowledge of boundary-layer behavior on continuous cylindrical surfaces and cylindrical surfaces of finite length will be reviewed.

THE LAMINAR BOUNDARY LAYER ON A CONTINUOUS CYLINDRICAL SURFACE

Approximate Solution

Consider steady, two-dimensional, incompressible flow on a continuous cylindrical surface moving with a constant velocity in a fluid medium at rest, as shown in Figure 1. The adopted frame of axes is stationary with its center point (at $x = 0$) located at the orifice. The positive x axis extends parallel to the surface and in the direction of its motion. The positive y axis extends radially from the solid surface ($y = 0$). The momentum equation for the boundary layer on a moving continuous cylindrical surface is (*19*)

$$\frac{d}{dx}\left(U_f^2\,\Theta\right) = \frac{2\pi a\,\tau_f}{(\rho/g_c)} \qquad (1)$$

where

$$\frac{d}{dx}\left(U_f^2\,\Theta\right) = \frac{d}{dx}\left\{\int_{y=0}^{y=\delta} u^2\,2\pi(a+y)\,dy\right\} \qquad (2)$$

The appropriate boundary conditions are

$$u = U_f \quad \text{at } y = 0$$

$$u = 0 \quad \text{at } y = \delta$$

Mark (*13*) and Glauert and Lighthill (*6*) have shown independently that the success of the integral momentum equation in determining the boundary-layer behavior depends to a large extent on how well the assumed velocity profile represents the conditions existing near the surface. These investigators showed that the appropriate velocity profile for a cylindrical surface of finite length is of a logarithmic type.

Mark has considered four logarithmic velocity profiles, the simplest profile of which is

$$\frac{u}{U_\infty} = \frac{1}{\alpha}\ln\left(1 + \frac{y}{a}\right) \qquad (3a)$$

or

$$\frac{u}{U_\infty} = \frac{\ln\left(\frac{a+y}{a}\right)}{\ln\left(\frac{a+\delta}{a}\right)} \qquad (3b)$$

For values $\delta << a$ the logarithmic profile reduces to a linear velocity profile for a flat surface of finite length

$$\frac{u}{U_\infty} = \hat{\eta} \qquad (4)$$

where $\hat{\eta} = y/\delta$. The other three logarithmic velocity profiles reduce, for values $\delta << a$, to second-, third-, and fourth-degree polynomials for the velocity profile for a flat surface of finite length. These more complicated velocity profiles are designed to satisfy more boundary conditions and to improve the accuracy of the approximate method of solution.

Glauert and Lighthill's logarithmic velocity profile is identical with Mark's profile given by Equations (3*a*) or (3*b*).

The results obtained with cylindrical surfaces of finite length suggest that the appropriate velocity profile for continuous cylindrical surfaces should be also logarithmic. The appropriate velocity profile should satisfy the following boundary conditions:

$$\frac{\partial^2 u}{\partial y^2} + \frac{1}{a}\frac{\partial u}{\partial y} = 0 \quad \text{at } y = 0$$

$$\frac{\partial u}{\partial y} = \frac{\partial^2 u}{\partial y^2} = 0 \quad \text{at } y = \delta$$

These conditions are determined from the differential boundary-layer equations for cylindrical surfaces (19) by setting $y = 0$ and $y = \delta$, respectively. The condition at the solid surface is more important than the condition near the edge of the boundary layer. The velocity profile assumed in this investigation for continuous cylindrical surfaces is

$$\frac{u}{U_f} = \left\{ 1 - \frac{1}{\beta} \ln\left(1 + \frac{y}{a} \right) \right\} \qquad (5)$$

where β is a function of x but not of y. This velocity profile satisfies the important boundary condition at $y = 0$ exactly. At $y = \delta$ the assumed velocity profile leads to the relations

$$\left(\frac{\partial u}{\partial y} \right)_{y=\delta} = -\frac{U_f}{\beta} \frac{1}{(a+\delta)}$$

and

$$\left(\frac{\partial^2 u}{\partial y^2} \right)_{y=\delta} = \frac{U_f}{\beta} \frac{1}{(a+\delta)^2}$$

which do not satisfy the second boundary condition. However both β and δ increase with increasing x, so that the second boundary condition is satisfied approximately at increasing distance from the origin. By contrast the fourth-degree polynomial used for the velocity profile on a continuous flat surface (20)

$$\frac{u}{U_f} = 1 - 2\hat{\eta} + 2\hat{\eta}^3 - \hat{\eta}^4 \qquad (6)$$

fails to satisfy the boundary condition at the solid surface. With this velocity profile

$$\frac{\partial^2 u}{\partial y^2} + \frac{1}{a}\frac{\partial u}{\partial y} = -\frac{2}{a}\frac{U_f}{\delta} \neq 0$$

Even though δ increases with increasing x, the radius a may be made arbitrarily small so that this condition is satisfied only for $a >> \delta$, $-(2/a)(U_f/\delta) \to 0$. Hence the velocity profile represented by Equation (6) is satisfactory only near the origin of the cylindrical surface, where δ is small compared with a and the surface may be considered as a wrapped flat sheet.

In the following development the assumed velocity profile is that given by Equation (5). This profile reduces to the linear profile

$$\frac{u}{U_f} = 1 - \hat{\eta} \qquad (7)$$

for $a >> \delta$.

With the assumed velocity profile the skin friction on the solid surface becomes

$$\tau_f = -\frac{\mu}{g_c}\left(\frac{\partial u}{\partial y} \right)_{y=0} = \frac{\mu U_f}{g_c \beta a} \qquad (8)$$

Substituting Equations (5) and (8) in Equations (1) and (2) and using the transformation $y = a(e^z - 1)$ one obtains

$$\frac{d}{dx}\left\{ \int_{z=0}^{z=\beta} U_f^2 \left[1 - \frac{z}{\beta} \right]^2 a^2 e^{2z}\, dz \right\} = \frac{\nu U_f}{\beta} \qquad (9)$$

since according to Equation (5) $z = \beta$ when $y = \delta$. Carrying out the operations on the left-hand side of Equation (9) one obtains

$$\left\{ \frac{2\beta e^{2\beta} - 2e^{2\beta}}{\beta^2} + \frac{2}{\beta} + \frac{2}{\beta^2} \right\} \frac{d\beta}{dx} = \frac{4}{U_f}\frac{\nu}{a^2} \qquad (10)$$

Equation (10) integrates to

$$\frac{4\nu x}{U_f a^2} = 2\int_{\beta=0}^{\beta} \left(\frac{\beta e^{2\beta} - e^{2\beta}}{\beta^2} + \frac{1}{\beta} + \frac{1}{\beta^2} \right) d\beta \qquad (11)$$

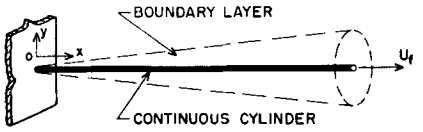

Fig. 1. The boundary layer on a moving continuous cylindrical solid surface.

with $\delta = 0$, or $\beta = 0$ at $x = 0$. The variation of β, and hence the variation of the skin friction τ_f with $(\nu x/U_f a^2)$, can be determined readily from Equation (11).

Equation (11) was evaluated by numerical methods and the results given in Table 1 in terms of ξ, where

$$\xi = 4\sqrt{\frac{\nu x}{U_f a^2}} = 4\frac{(x/a)}{(N_{Re})_x^{1/2}} = 8\frac{(N_{Re})_x^{1/2}}{(N_{Re})_d}$$

$$(N_{Re})_x = \frac{U_f x}{\nu}$$

$$(N_{Re})_d = \frac{U_f d}{\nu}$$

Hence the parameter β is a function of the length Reynolds number and the length-to-diameter ratio.

The primary characteristic boundary-layer parameters can now be determined readily with Equation (5) and the established dependence of β on ξ. These parameters are

$$\frac{\Theta}{\pi a^2} = \frac{1}{\pi a^2 U_f^2}\int_{y=0}^{y=\delta} u^2 2\pi(a+y)\,dy \qquad (12a)$$

or

$$\frac{\Theta}{\pi a^2} = \frac{e^{2\beta}-1}{2\beta^2} - \frac{1}{\beta} - 1 \qquad (12b)$$

The dimensionless momentum area is related to the momentum thickness by

$$\Theta = \pi\left[(a+\theta)^2 - a^2\right] \qquad (13)$$

and

$$\frac{\Delta}{\pi a^2} = \frac{1}{\pi a^2 U_f}\int_{y=0}^{y=\delta} u\, 2\pi(a+y)\,dy \qquad (14a)$$

or

$$\frac{\Delta}{\pi a^2} = \frac{e^{2\beta} - 2\beta - 1}{2\beta} \qquad (14b)$$

The dimensionless displacement area is related to the displacement thickness by

$$\Delta = \pi\left[(a+\delta^*)^2 - a^2\right] \qquad (15)$$

The dimensionless boundary-layer thickness can be determined readily from Equation (5) with $y = \delta$ at $u/U_f = 0$; the result is

$$\frac{\delta}{a} = e^{\beta} - 1 \qquad (16)$$

The dimensionless momentum area $\Theta/\pi a^2$, displacement area $\Delta/\pi a^2$, and boundary-layer thickness δ/a were evaluated as a function of β. The results are given in Table 1* and plotted as a function of ξ in Figure 2.

The secondary characteristic boundary-layer parameters are obtained as follows:

$$C'_f = \frac{g_c \tau_f}{1/2(\rho U_f^2)} = \frac{2\nu}{\beta a U_f} \qquad (17)$$

the dimensionless local coefficient of skin friction

$$D = 2\pi a \int_{x=0}^{x=L} \tau_f dx = \frac{\rho}{g_c} U_f^2 \Theta \qquad (18)$$

the total drag on the continuous surface

$$C_f = \frac{g_c D}{(1/2)\rho\,(2\pi a L) U_f^2} = \left(\frac{\Theta}{\pi a^2} \right) \frac{a}{L} \qquad (19)$$

the dimensionless coefficient for total drag, and

$$q = \Delta U_f \qquad (20)$$

the pumping action or total volume of fluid entrained by the moving surface.

Of interest also is the ratio of the characteristic parameters for the boundary layer on a continuous cylindrical surface to the characteristic parameters

* For all total quantities such as $\Theta/\pi a^2$, the length x in ξ represents the total exposed length of the surface.

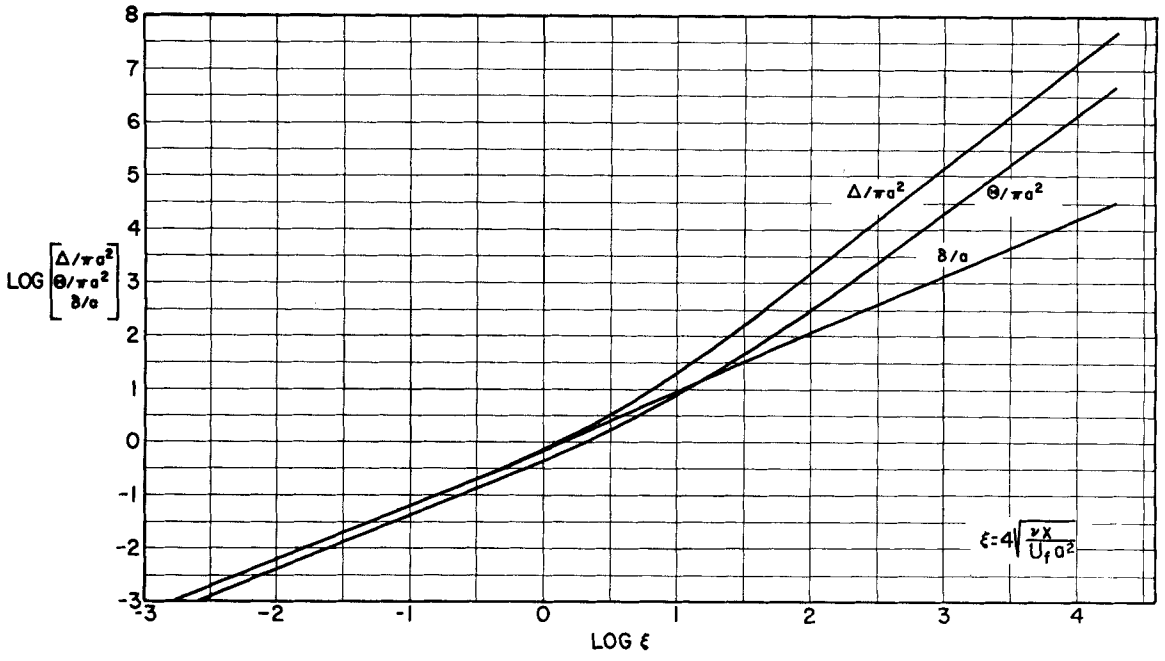

Fig. 2. Boundary-layer parameters.

of the boundary layer on a continuous flat surface of equivalent area. The momentum thickness, displacement thickness, and boundary-layer thickness for a continuous flat surface are determined by relations of the form (20)

$$\theta_p = C_\theta \sqrt{\frac{\nu x}{U_f}}$$

$$\delta_p^* = C_\delta^* \sqrt{\frac{\nu x}{U_f}}$$

$$\delta_p = C_\delta \sqrt{\frac{\nu x}{U_f}}$$

The ratio of the drag, pumping action, and boundary-layer thickness on a continuous cylindrical surface to the corresponding parameters on a continuous flat surface of equivalent area becomes

$$\frac{D}{D_p} = \frac{2(\Theta/\pi a^2)}{C_\theta\, \xi} \qquad (21)$$

$$\frac{q}{q_p} = \frac{2(\Delta/\pi a^2)}{C_\delta^*\, \xi} \qquad (22)$$

$$\frac{\delta}{\delta_p} = \frac{4(\delta/a)}{C_\delta\, \xi} \qquad (23)$$

For a linear velocity profile to which the logarithmic profile degenerates for $a \to \infty$ the constants assume the values

$$C_\theta = 0.817$$
$$C_\delta^* = 1.225$$
$$C_\delta = 2.449$$

In a sense Equations (21), (22), and (23) may be considered as representing the effect of surface curvature on the boundary-layer parameters. These equations were evaluated by the use of Table 1, and the results are given in Table 2.

Table 1. Boundary-Layer Parameters

log ξ	β	log (Θ/πa²)	log (Δ/πa²)	log (δ/a)
−3.0880	0.0005	−3.4770	−3.3009	−3.3009
−2.7869	0.001	−3.1759	−2.9997	−2.9998
−2.0873	0.005	−2.4760	−2.2996	−2.2999
−1.7856	0.01	−2.1739	−1.9971	−1.9978
−1.0807	0.05	−1.4662	−1.2864	−1.2901
−0.7724	0.1	−1.1540	−0.9706	−0.9781
−0.0113	0.5	−0.3599	−0.1437	−0.1879
0.3757	1.0	0.0774	0.3413	0.2351
0.8781	2.0	0.7160	1.0934	0.8054
1.2945	3.0	1.3226	1.8200	1.2807
1.6939	4.0	1.9632	2.5700	1.7291
2.0926	5.0	2.6428	3.3428	2.1685
2.4941	6.0	3.3539	4.1342	2.6047
2.8993	7.0	4.0888	4.9340	3.0397
3.3076	8.0	4.8415	5.7446	3.4742
3.7184	9.0	5.6078	6.5621	3.9086
4.1325	10.0	6.3849	7.3849	4.3429

Rayleigh's Problem

Rayleigh's method may be used to obtain a rough solution to the boundary-layer behavior on continuous cylindrical surfaces. In this method the approach is taken that all convection takes place at the constant velocity U_f which simplifies the convection terms in the momentum equation. Rayleigh's problem (17) involves the case of the flow near an infinitely long cylinder which is suddenly accelerated from rest and moves in its own plane with a constant velocity U_o. The solution to Rayleigh's problem may be applied (20) to the moving continuous cylindrical surface considered here by considering the time from the start-up of motion as the time interval during which a solid particle of the surface is subjected to drag.

Rayleigh's problem for a cylindrical surface has been considered by a number of investigators (3). In Figure 3 are plotted the dimensionless momentum and displacement areas as a function of ξ for comparison with the results obtained in the previous section. In this method the momentum and displacement areas are equal. The numerical results determined by Rayleigh's method are taken from Jaeger (10).

Discussion

The laminar boundary-layer behavior on a continuous cylindrical surface has been determined also by as-

suming that the velocity profile in the boundary layer is represented by a fourth-degree polynomial [Equation (6)]. Evaluation of the characteristic boundary-layer parameters based on this profile leads to the following results for the total drag and the boundary-layer thickness:

$$\frac{D}{D_p} = \phi\ (\xi) \qquad (24)$$

$$\frac{\delta}{\delta_p} = \psi\ (\xi) \qquad (25)$$

where ϕ and ψ equal 1.0 at $\xi = 0$, and $\phi = 2.18$, $\psi = 0.361$ at $\xi = 80$.

The effect of surface curvature on the total drag computed on the basis of the parabolic velocity profile is considerably smaller than that computed on the basis of the logarithmic velocity profile as shown by comparison with Table 2. The reasonable agreement obtained between the results computed on the basis of the logarithmic velocity profile and Rayleigh's method, as shown in Figure 3, leads to the conclusion that the parabolic velocity profile does not represent accurately the conditions in the boundary layer on cylindrical surfaces. Note also that according to Equation (25) the boundary-layer thickness on a continuous cylindrical surface is smaller than that on an equivalent flat surface. This is contrary to the results presented in Table 2. Preliminary partial numerical solution of the differential boundary-layer equations [Equations (3) and (4), reference *19*] by numerical methods substantiates the trend of the results given in Table 2.

The effect of surface curvature on the characteristic boundary-layer parameters is determined by the value of the function ξ. As shown in Table 2 this effect becomes significant for $\xi > 0.1$ and increases rapidly with increasing values of ξ. Note however that comparison of the boundary-layer behavior on a cylindrical surface with the boundary-layer behavior on an equivalent flat surface of very large width is somewhat misleading. Batchelor (*2*) and other investigators (*7, 8, 9*) found, for Rayleigh's problem, that the drag on narrow flat strips is not very much different from the drag on circular cylinders of equal periphery. The high drag on the narrow flat strips is due to the presence of the edges.

The laminar boundary-layer behavior on cylindrical surfaces of finite length has been studied by a number of investigators (*6, 12, 13, 16, 18, 21, 22*). Glauert and Lighthill (*6*) present recommended curves, expected to be correct within about 2%, for the variation along the cylinder of the skin friction, boundary-layer displacement area, and momentum area. The curves for the displacement and momentum areas are reproduced in Figure 3 for comparison with the results obtained for the continuous cylindrical surfaces. For low values of ξ, when the cylindrical surfaces can be treated as equivalent flat surfaces, the momentum area or drag on the continuous surface is higher than that on the surface of finite length (see also Table 2, reference *20*). This trend is reversed for higher values of ξ. The variation of the displacement area or pumping action with ξ is the reverse of the variation of the momentum area or drag with ξ. Another important difference between the boundary-layer behavior on a continuous cylindrical surface and a cylindrical surface of finite length is the variation of the boundary-layer thickness with ξ. For a continuous cylindrical surface the ratio δ/δ_p increases with increasing ξ, as shown in Table 2. Glauert and Lighthill's results (6) indicate that the ratio δ/δ_p for a cylindrical surface of finite length decreases with increasing ξ.

THE TURBULENT BOUNDARY LAYER ON A CONTINUOUS CYLINDRICAL SURFACE

Approximate Solution

The behavior of turbulent boundary layers is best investigated by approximate methods. With a suitable empirical relation for the velocity profile in the boundary layer, the momentum integral equation yields the sought characteristic parameters of the boundary layer. In a previous paper (*20*) this method was used to determine the boundary-layer behavior on a continuous flat surface, with fairly satisfactory results. It remains to be seen whether equally satisfactory results can be obtained for a continuous cylindrical surface.

In the following analysis the assumption will be made that the velocity profile in the turbulent boundary layer on a continuous cylindrical surface is the same as the profile on a continuous flat surface and is represented by the relation

$$\frac{u}{U_f} = 1 - \hat{\eta}^{1/7} \qquad (26)$$

The assumption will also be made that the shear stress at the solid surface is given by

$$\frac{\tau_f}{(\rho/g_c)U_f^2} = 0.0225\left(\frac{\nu}{U_f\delta}\right)^{1/4} \qquad (27)$$

This is the same relation used for determining the turbulent boundary layer on a continuous flat surface and a flat plate of finite length with zero pressure gradient along the surface.

The momentum area is determined readily from Equations (12*a*) and (26); hence

$$\Theta = 2\pi\left(\frac{1}{36}a\,\delta + \frac{1}{240}\delta^2\right) \qquad (28)$$

Differentiation of Equation (28) with respect to x and substitution of the result together with Equation (27) in Equation (1) results in

$$(\zeta^{1/4} + 0.3\,\zeta^{5/4})\,d\zeta = 0.81\left(\frac{\nu}{U_f a}\right)^{1/4} d\left(\frac{x}{a}\right) \qquad (29)$$

where $\zeta = \delta/a$. Integration of Equation (29) from the initial value $\zeta = 0$ at $x/a = 0$ results in the following equation for the boundary-layer thickness:

$$\zeta^{5/4} + 0.167\,\zeta^{9/4} = 1.01\,\frac{x}{a}\left(\frac{\nu}{U_f a}\right)^{1/4} \qquad (30)$$

Equation (30) can also be expressed as

$$\zeta = \kappa\,\lambda^{4/5} \qquad (31)$$

where $\lambda = \left[\left(\frac{x}{a}\right)\left(\frac{\nu}{U_f a}\right)^{1/4}\right]$

and κ is related to λ as follows:

$\lambda^{1/5}$	κ
0	1.000
0.5	0.987
1.0	0.891
1.5	0.682
2.0	0.500
2.5	0.371
3.0	0.281
3.5	0.220
4.0	0.177
5.0	0.122
6.0	0.088
7.0	0.068

The total drag on the continuous cylindrical surface is obtained from Equations (18) and (28):

$$D = \frac{\rho}{g_c}\,U_f^2\,2\pi a\delta\left(\frac{1}{36} + \frac{1}{240}\,\frac{\delta}{a}\right) \qquad (32)$$

In the limit of $\zeta \to 0$ Equations (30) and (32) reduce to the corresponding parameters for a continuous flat surface (*20*).

The ratio of the boundary-layer thickness on a continuous cylindrical surface to the boundary-layer thickness on an equivalent flat surface is simply

$$\frac{\delta}{\delta_p} = \kappa \qquad (33)$$

The ratio of the drag on the continuous cylindrical surface to the drag

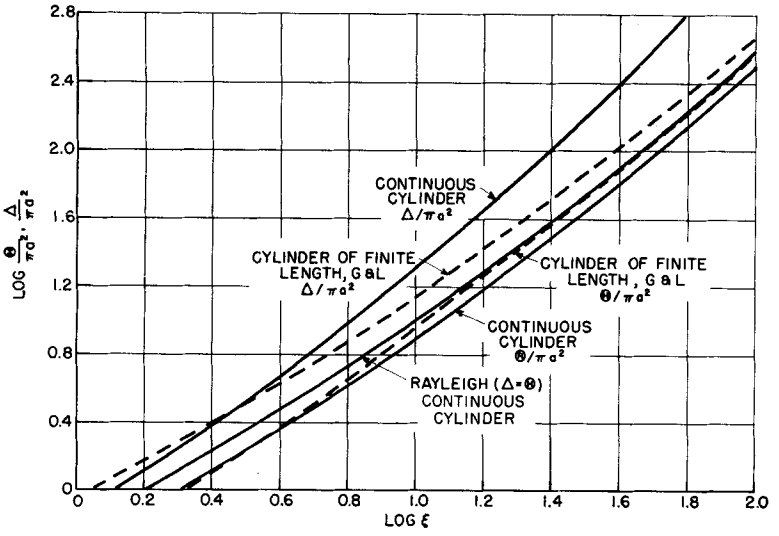

Fig. 3. Boundary-layer parameters for cylindrical surfaces.

on an equivalent continuous flat surface is

$$\frac{D}{D_p} = (1 + 0.152\zeta)\,\kappa \qquad (34)$$

which is evaluated below:

$\lambda^{1/5}$	D/D_p
0	1.00
0.5	1.00
1.0	1.01
1.5	1.05
2.0	1.11
2.5	1.18
3.0	1.25
3.5	1.33
4.0	1.40
5.0	1.54
6.0	1.65
7.0	1.75

The remaining boundary-layer parameters can be determined readily from the established relationships.

Discussion

The above analysis of the turbulent boundary-layer behavior on cylindrical surfaces does not lead to satisfactory results. First, in accordance with Equation (33), the boundary-layer thickness on a cylindrical surface is smaller than the boundary-layer thickness on an equivalent flat surface. The results obtained from the more reliable analysis for the laminar boundary layer (Table 2) indicate that the opposite is true. Since it is unlikely that the laminar and turbulent boundary layers will behave so differently, this leads to the conclusion that Equation (33) is not reliable. Second, in accordance with Equation (34), the drag on a cylindrical surface is only about twice the drag on an equivalent flat surface for the highest values of $\lambda^{1/5}$ investigated. Hence the ratio D/D_p computed from Equation (34) is smaller than that predicted from Table 2 for the laminar boundary layer at equivalent flow conditions. This leads to the conclusion that Equation (34) also is not reliable. The unsatisfactory results obtained from the analysis of the turbulent boundary-layer behavior are due partly to the use of the same velocity profile for a cylindrical surface and a flat surface. This has been shown conclusively to be the case for the laminar boundary layer.

The turbulent boundary layer on a cylindrical surface of finite length has been studied by a number of investigators (*5*, *11*, and *18*). Eckert (*5*) indicates that there are three courses that may be followed in studying the turbulent boundary-layer behavior on a cylindrical surface by approximate methods:

1. The momentum thickness and velocity profile are the same for the cylinder and the plate.

Table 2. Surface Curvature Effect on Boundary-Layer Parameters

$\log \xi$	D/D_p	q/q_p	δ/δ_p
−3.0880	1.000	1.000	1.000
−2.7869	1.000	1.000	1.000
−2.0873	1.001	1.001	1.001
−1.7856	1.002	1.003	1.002
−1.0807	1.008	1.017	1.008
−0.7724	1.017	1.034	1.017
−0.0113	1.097	1.204	1.087
0.3757	1.232	1.508	1.181
0.8781	1.686	2.681	1.381
1.2945	2.613	5.475	1.582
1.6939	4.553	12.27	1.771
2.0926	8.693	29.05	1.945
2.4941	17.73	71.28	2.106
2.8993	37.89	176.8	2.256
3.3076	83.73	446.6	2.397
3.7184	189.8	1139.4	2.530
4.1325	437.9	2919.5	2.651

2. The law of shear stress and velocity profile are the same for the cylinder and the plate.

3. The boundary-layer thickness and velocity profile are the same for the cylinder and the plate.

The first course leads to a smaller boundary-layer thickness for the cylinder than for the plate. Eckert adopted the second course and determined the characteristic boundary-layer parameters accordingly. The course adopted in the present investigation on continuous cylindrical surfaces is the same course adopted by Eckert for cylindrical surfaces of finite length. Therefore Eckert's results are subject to the same uncertainty as the results of the present investigation on the turbulent boundary-layer behavior.

Jakob and Dow (*11*) adopted the third course. Their results, for the same velocity profile, give too high values for the drag.

This discussion leads to the conclusion that the results of the analysis of the turbulent boundary-layer behavior on continuous cylindrical surfaces are unreliable. The same is true for the published results for turbulent boundary layers on cylindrical surfaces of finite length. Clearly the problem must be solved by experimentation.

COMPARISON OF THEORETICAL PREDICTIONS AND EXPERIMENTAL OBSERVATIONS

There are no published measurements of drag or any of the characteristic boundary-layer parameters on continuous cylindrical surfaces. Since the boundary-layer behavior on continuous cylindrical surfaces is somewhat similar to that on cylindrical surfaces of finite length, measurements on surfaces of finite length may be used to estimate the reliability of the results of this investigation. Unfortunately the published measurements on cylindrical surfaces of finite length are limited, making any comparison between theory and experiment uncertain.

Richmond (*18*) reports some measurements of the velocity distribution and skin-friction coefficients on four cylinders at subsonic and hypersonic speeds. His experimental arrangement does not permit correlation of the measurements as a function of the distance x from the leading edge. The measurements are therefore reported as a function of a momentum thickness Reynolds number.

Richmond was unable to obtain a steady symmetrical laminar boundary layer at subsonic speeds. His measurements of the hypersonic laminar boundary layer are in reasonable agreement with Glauert and Lighthill's theory as

extended by Coles (*18*) to compressible flow. This was expected, since Glauert and Lighthill's results were determined from a nearly exact solution of the boundary-layer equations for cylindrical surfaces.

An attempt was made to predict Richmond's results for the subsonic turbulent boundary layer by using Eckert's theory. The author finds surprisingly good agreement between Eckert's theory and Richmond's results. This agreement however leads to the conclusion that the turbulent drag on a cylindrical surface is lower than the laminar drag on the surface for the same flow.

Clearly additional measurements of the turbulent boundary-layer behavior on cylindrical surfaces are needed.

Further comparison between theory and experiment can be made indirectly by considering results of mass and heat transfer measurements (*1, 4, 14, 15*) on cylindrical surfaces and using the *j*-factors of the Chilton-Colburn analogy. These measurements indicate that the turbulent drag on fine cylindrical surfaces is higher than the laminar drag on the same surfaces, as would be expected.

SUMMARY

Laminar Boundary Layer

The characteristic parameters of the laminar boundary layer on a continuous cylindrical surface can be determined from Equations (12*b*), (14*b*), (16), (17), (18), (19), and (20), in conjunction with Table 1 or Figure 2.

Turbulent Boundary Layer

The derived theoretical relations for the turbulent boundary layer on a continuous cylindrical surface do not predict correctly the effect of surface curvature on the skin friction and other parameters. The turbulent boundary-layer behavior on continuous cylindrical surfaces, and cylindrical surfaces of finite length, can best be investigated experimentally.

An estimate of the turbulent skin-friction coefficient on continuous cylindrical surfaces can be obtained from published heat transfer measurements by use of the momentum heat transfer analogy.

NOTATION

a = radius of cylindrical surface, ft.

C = constant, dimensionless

C_f' = coefficient for local skin friction, dimensionless

C_f = coefficient for total skin friction, dimensionless

D = drag, lb.-force

d = diameter of cylindrical surface, ft.

g_c = conversion factor, 32.2 (lb.) (ft.)/(lb.-force) (sec.)^2

L = exposed length of cylindrical surface, ft.

q = volumetric flux, cu. ft./sec.

$(N_{Re})_d$ = $U_f d/\nu$, $U_\infty d/\nu$ = Reynolds number based on cylinder diameter, dimensionless

$(N_{Re})_x$ = $U_f x/\nu$, $U_\infty x/\nu$ = Reynolds number based on axial length, dimensionless

U_f = velocity of continuous cylindrical surface, ft./sec.

U_o = velocity of suddenly accelerated, infinitely long cylindrical surface, ft./sec.

U_∞ = velocity of potential flow over stationary cylindrical surface of finite length, ft./sec.

u = fluid velocity component in the x direction, ft./sec.

x, y = cylindrical coordinates, ft.

z = dimensionless parameter

Greek Letters

α = function of x, dimensionless parameter

β = function of x, dimensionless parameter

Δ = displacement area, sq. ft.

δ = boundary-layer thickness, ft.

δ^* = displacement thickness, ft.

ζ = δ/a = dimensionless boundary-layer thickness

η = y/δ = dimensionless parameter

Θ = momentum area, sq. ft.

θ = momentum thickness, ft.

$\kappa(\lambda)$ = δ/δ_p = boundary-layer thickness ratio for turbulent boundary layer, dimensionless

λ = $[(x/a)(\nu/U_f a)^{1/4}]$ = parameter for turbulent boundary layer, dimensionless

μ = fluid viscosity, (lb.)/(ft.) (sec.)

ν = μ/ρ = kinematic fluid viscosity, sq. ft./sec.

ξ = $4\sqrt{\nu x/U_f a^2}$ = parameter for laminar boundary layer, dimensionless

ρ = fluid density, lb./cu. ft.

τ_f = shear stress on continuous cylindrical surface, lb.-force/sq. ft.

$\phi(\xi)$ = D/D_p = drag ratio for laminar boundary layer, dimensionless

$\psi(\xi)$ = δ/δ_p = boundary-layer thickness ratio for laminar boundary layer, dimensionless

Subscripts

d = diameter of cylindrical surface

p = continuous flat surface

x = axial distance

δ = boundary-layer thickness

δ^* = displacement thickness

θ = momentum thickness

LITERATURE CITED

1. Anantanarayanan, R., and A. Ramachandran, *Paper No. 57-A-100,* presented at the Annual Meeting of the Am. Soc. of Mech. Engrs., New York (Dec., 1957).
2. Batchelor, G. K., *Quart. J. Mech. Appl. Math.*, **7**, 179 (1954).
3. Carslaw, H. S., and J. C. Jaeger, "Conduction of Heat in Solids," Section 127, Oxford Univ. Press, London, England (1947).
4. Christian, W. J., and S. P. Kezios, "Experimental Investigation of Mass Transfer by Sublimation from Sharp-Edged Cylinders in Axisymmetric Flow with Laminar Boundary Layer," Preprints of Papers for the 1957 Heat Transfer and Fluid Mechanics Institute, Pasadena, California, published by Stanford University Press, Stanford, Calif.
5. Eckert, H. U., *J. Aeronaut. Sci.*, **19**, 23 (1952).
6. Glauert, M. B., and M. J. Lighthill, "International Symposium on Boundary Layer Effects in Aerodynamics," Vol. 2, p. 1, Philosophical Library, New York (1957); *Proc. Roy. Soc. (London)*, **230A**, 188 (1955).
7. Hasimoto, H., *J. Phys. Soc. Japan*, **9**, 611 (1954).
8. *Ibid.*, **10**, 397 (1955).
9. Howarth, L., *Proc. Camb. Phil. Soc.*, **46**, 127 (1950).
10. Jaeger, J. C., *Proc. Roy. Soc.*, **61A**, 223 (1942); J. C. Jaeger, and M. Clarke, *ibid.*, **61A**, 229 (1942).
11. Jakob, Max, and W. M. Dow, *Trans. Am. Soc. Mech. Engrs.*, **68**, 123 (1945).
12. Kelly, H. R., *J. Aeronaut. Sci.*, **21**, 634 (1954).
13. Mark, R. M., "Laminar Boundary Layers on Slender Bodies of Revolution in Axial Flow," Memorandum No. 21, Guggenheim Aeronautical Laboratory, Calif. Inst. Technol. (July 30, 1954).
14. Mueller, A. C., *Trans. Am. Inst. Chem. Engrs.*, **38**, 613 (1942).
15. Petrou, L., *Comp. Rend. Acad. Sci.*, **239**, 1187 (1954).
16. Probstein, R. F., and D. Elliott, *J. Aeronaut. Sci.*, **23**, 208 (1956).
17. Rayleigh, Lord, *Phil. Mag.*, **21**, 697 (1911).
18. Richmond, R. L., "Experimental Investigation of Thick Axially Symmetric Boundary Layers on Cylinders at Subsonic and Hypersonic Speeds," Memorandum No. 39, Guggenheim Aeronautical Laboratory, Calif. Inst. Technol. (June 20, 1957).
19. Sakiadis, Byron C., *A.I.Ch.E. Journal*, **7**, No. 1, p. 26 (1961).
20. *Ibid.*, No. 2, p. 221 (1961).
21. Seban, R. A., and R. Bond, *J. Aeronaut. Sci.*, **18**, 671 (1951).
22. Stewartson, K., *Quart. Appl. Math.*, **13**, 113 (1955).

Manuscript received January 2, 1959; revision received November 21, 1960; paper accepted November 23, 1960.